PHYSICAL REVIEW C VOLUME 49, NUMBER 5 MAY 1994

Neutron halo effect on direct neutron capture and photodisintegration

T. Otsuka,[1,2] M. Ishihara,[1,2] N. Fukunishi,[1,2] T. Nakamura,[1,2] and M. Yokoyama[1]
[1] *Department of Physics, University of Tokyo, Hongo, Bunkyo-ku, Tokyo 113, Japan*
[2] *RIKEN, 2-1, Hirosawa, Wako, Saitama, 351-01, Japan*

(Received 2 September 1993)

A novel effect of the neutron halo formation is presented for the direct radiative neutron capture where a p-wave neutron is captured into an s orbit with neutron halo by emitting an $E1$ γ ray. As an example, an enormous enhancement is demonstrated for the cross section of $^{12}\mathrm{C}(n,\gamma)^{13}\mathrm{C}(1/2^+)$ at low energy in excellent agreement with a recent experiment. The S factor of the final state is evaluated. The inverse process, i.e., photodisintegration is discussed for an example of ^{11}Be. A sharp but nonresonant peak near the threshold is obtained as a result of the neutron halo in its anomalous ground state.

PACS number(s): 25.40.Lw, 21.10.Gv, 21.10.Jx, 25.70.De

The neutron halo is known to be one of the most prominent and exotic effects seen in the ground states of some unstable nuclei. This phenomenon has been discovered by Tanihata *et al.*, opening a new page of physics with radioactive nuclear beams [1]. Later Hansen and Jonson made an analysis of this phenomenon in terms of a small separation energy [2]. As already mentioned in Ref. [3], referring to it as *halo universality*, the neutron halo should not be limited to exotic nuclei, and in fact should be seen in excited states of a large number of nuclei on and off the β stability line, for instance, the first $\frac{1}{2}^+$ state of ^{13}C. However, it has remained extremely difficult to carry out experiments on the halo structure in excited states. We shall demonstrate that the direct radiative neutron capture offers an extremely sensitive means to study the halo structure.

The direct neutron capture into the $2s_{1/2}$ orbit is discussed for the reaction $^{12}\mathrm{C}(n,\gamma)\,^{13}\mathrm{C}(1/2^+)$, as an example. This neutron capture is associated with $E1$ γ ray emission, and the capture cross section shows, because of the halo structure of the $\frac{1}{2}^+$ state, a novel and enormous enhancement for the incoming neutron with kinetic energy from zero to a few MeV. The present low-energy direct capture is of indispensable significance as a new and presently unique tool for investigating the halo structure particularly in excited states. It is also of particular importance in astrophysical issues, for instance, the inhomogeneous Big Bang model, the neutron poison, etc. Thus, the direct neutron capture bridges the physics of the neutron halo to the astrophysics. The incoming neutron is in a p wave in the present case, because it is captured into the s orbit through the $E1$ process. This highlights a major difference from the usual capture process where an s-wave neutron is captured into a bound p orbit. The inverse process, i.e., photodisintegration is also discussed. A sharp but nonresonant peak near the threshold is presented for the example of ^{11}Be, giving rise to a test stone of the neutron halo in its anomalous ground state.

The capture process is treated in the plane wave Born approximation. The relative momentum between the incoming neutron and the target nucleus is denoted as $\hbar\mathbf{k}$ in the center-of-mass (c.m.) frame. The kinetic energy of this relative motion is dentoed as E. The target nucleus has the mass number $A-1$ with Z protons and $N-1$ neutrons, so that the nucleus after the capture has Z protons and N neutrons ($A = Z + N$).

The cross section is calculated by [4]

$$\sigma_{lm} = \frac{8\pi(l+1)}{l[(2l+1)!!]^2}\left(\frac{\omega}{c}\right)^{2l+1}\frac{1}{\hbar\nu}|Q^2_{lm}|, \tag{1}$$

where Q_{lm} is the transition matrix element as discussed below, l and m are the angular momentum and its z projection of the emitted photon, $\hbar\omega$ implies the energy of the photon, and ν denotes the relative velocity. We choose the z axis of a Cartesian coordinate frame as being the direction $\mathbf{k}$ [i.e., $\mathbf{k} = (0,0,k)$]. We consider, in the following, the case in which the incoming neutron is captured into the $2s_{1/2}$ orbit on the top of the 0^+ ground-state core of ^{12}C by radiating $E1$ γ ray. As will be shown shortly, the $E1$ transition from a continuum state to the $2s$ orbit state is enhanced for low E, if the halo is formed in the capturing s orbit. Other multipole transitions are enhanced similarly due to the larger radius, but their magnitudes are still far below $E1$. Because of the centrifugal barrier, the single-neutron halo can hardly be formed in an orbit, if its orbital angular momentum is greater than zero. Therefore, the combination of the $E1$ radiative capture and the s orbit as the capturing state is probably unique for the enhancement of the direct capture cross section at low E.

The matrix element Q_{lm} (l=1) is given in the present case by

$$Q_{1m} = \langle ^{13}\mathrm{C}(\tfrac{1}{2}^+)|T^{(E1)}|^{12}\mathrm{C}(0^+)\mathbf{k}\rangle, \tag{2}$$

where $|\mathbf{k}\rangle$ denotes the incoming plane wave, and $T^{(E1)}$ stands for the $E1$ transition operator. The wave function of ^{13}C can be written in terms of a linear combination of products of the core part and the part representing the relative motion between the core and last neutron (i.e., captured neutron). The c.m. and relative coordinates are denoted, respectively, as $\mathbf{R}$ and $\mathbf{r}$. The $E1$ transition operator becomes

$$T^{(E1)} = e\sqrt{3/4\pi}\{Z\mathbf{R} - (Z/A)\mathbf{r}\}. \quad (3)$$

Since we are not interested in the c.m. motion, only the second term on the right-hand side of Eq. (3) is considered in the following calculations.

The wave function of the first $\frac{1}{2}^+$ state of ^{13}C can be decomposed as

$$|^{13}\mathrm{C}(\tfrac{1}{2}^+)_1\rangle = \zeta_1|^{12}\mathrm{C}(0^+{}_1) \times (2s_{1/2})_\nu\rangle + \cdots, \quad (4)$$

where the ζ's are amplitudes, $|^{12}\mathrm{C}(0^+{}_1)\rangle$ stands for the 0^+ ground state of the ^{12}C core, $(\ )_\nu$ means an orbit for the last neutron (i.e., its relative motion). The first term on the right-hand side of Eq. (4) is the primary component [3,5,6], and yields a predominant contribution to the capture process over the other terms because the core can remain unchanged through this process. We then keep only the first term of the right-hand side of Eq. (4). In this case, the core produces no contribution to the $E1$ matrix element, as being the spectator. One then obtains

$$Q_{1m} = -\delta_{m,0}\zeta_1\sqrt{3}ie(Z/A)\int_0^\infty dr\, r^3 R(r) j_1(kr), \quad (5)$$

where $r \equiv |\mathbf{r}|$, and $R(r)$ is the $2s_{1/2}$ radial wave function. In Eq. (5), $j_1(kr)$ denotes a spherical Bessel function, and arises because we are extracting the p wave component from $e^{i\mathbf{k}\cdot\mathbf{r}}$. Since Eq. (5) is basically a Fourier transformation, Q_{10} becomes large for small k if $R(r)$ has a slowly damping tail, or halo. Note that $\zeta_1 = 1$ is used in the following calculations.

As shown later, the tail part of $R(r)$ is important in this study, and should be determined accurately. It is known that, at $r \to \infty$, $R(r) \propto e^{-\mu r}/r$ where $\mu \equiv \sqrt{2MS_n}/\hbar$ with S_n and M being the separation energy and the reduced mass, respectively. On the other hand, the inner part of the wave function is not very relevant to the present study. We therefore use the $2s_{1/2}$ wave function of a square well potential the depth of which is adjusted so that the corresponding energy eigenvalue is equal to $-S_n$. Because the square well potential does not have diffuseness, the potential radius, r_0, is set to a value larger than the usual nuclear radius. We use the observed value $S_n = 1.86$ MeV, and take $r_0 = 4$ fm as discussed later. This wave function is denoted as $R_W(r)$, and its explicit form is

$$R_W(r) = \alpha\, \sin(\kappa r)/r \quad \text{for } 0 \le r < r_0 \quad (6a)$$

and

$$R_W(r) = \beta e^{-\mu r}/r \quad \text{for } r_0 \le r < \infty, \quad (6b)$$

where α and β denote amplitudes, and $\kappa \equiv \sqrt{2M(V - S_n)}/\hbar$ with V ($V > 0$) being the potential depth. The cross section calculated from $R_W(r)$ is denoted as σ_W, and is shown in Figs. 1(a) and 1(b), demonstrating an excellent agreement to a recent experiment by

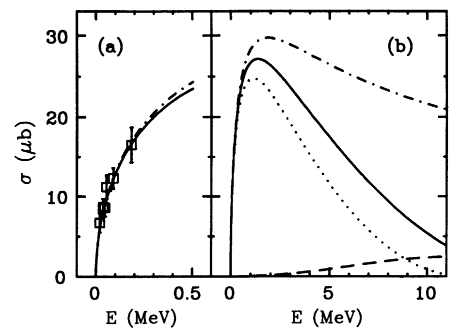

FIG. 1. Direct neutron capture cross section to the first $\frac{1}{2}^+$ state of ^{13}C as a function of the relative kinetic energy E; (a) is enlargement of the low-energy part of (b). Points are experimental [7]. The solid and dot-dashed lines are obtained, respectively, from the R_W [Eq. (6)] and $R_{\rm SY}$ [Eq. (7)] wave functions. The dotted and dashed lines in (b) are calculated, respectively, from R_W and $R_{\rm HO}$ with the orthogonalization (see the text).

Ohsaki *et al.* for $E \approx 10$ keV$\sim$200 keV [7]. The sharp increase in the low energy region is perfectly reproduced.

The integrand in Eq. (5) is the product of a function $Q(r) \equiv r^3 R(r)$ and a Bessel function $j_1(kr)$. Figure 2 shows the values of $Q(r)$ for several $R(r)$'s. For $Q_W(r) \equiv r^3 R_W(r)$, one finds a huge bump around 7 fm. Equation (5) depends on k of $j_1(kr)$. For $E = 2$ MeV ($E \equiv \hbar^2k^2/2M$), $j_1(kr)$ shows the first and largest peak around $r = 7$ fm which overlaps with the above peak of $Q_W(r)$. Thus, the cross section becomes largest around $E = 2$ MeV. For smaller E (or k), the first peak of $j_1(kr)$ moves outward, and only the further outer part of $R(r)$ becomes relevant, yielding a smaller cross section as seen in Fig. 1. Thus, for $R_W(r)$, only Eq. (6b) has major significance to the present cross section below $E = 2$ MeV. We then ignore details of the inner part in Eq. (6a) and approximate the whole wave function by Eq. (6b). Thus, the "scaled-Yukawa" wave function, denoted $R_{\rm SY}(r)$, is introduced.

By using an approximate expression of β for a small value of S_n [2], one can define

$$R_{\rm SY}(r) \equiv \frac{\exp(\mu r_0)}{\sqrt{1+\mu r_0}}\sqrt{2\mu}e^{-\mu r}/r \quad \text{for } 0 < r < \infty. \quad (7)$$

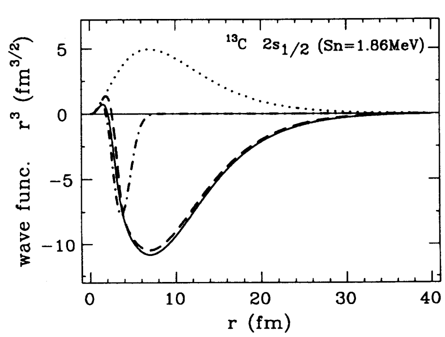

FIG. 2. The $2s_{1/2}$ radial wave functions for ^{13}C multiplied by r^3, as a function of the radial coordinate r. The solid, dotted, and dot-dashed lines correspond to R_W, R_Y, and $R_{\rm HO}$, respectively. The dashed line is obtained from the VSM [3].

Since $R_{\rm SY}(r)$ does not have a correct normalization, it makes sense only for certain matrix elements dominated by the wave-function tails, for instance, the present one. The normalized Yukawa function $R_Y(r) \equiv \sqrt{2\mu}e^{-\mu r}/r$ has an excessive fraction of the probability in the inner part of the nucleus, and hence has too small an amplitude in the outer region. The resultant cross section, denoted by σ_Y, becomes too small for low E. Thus, $R_{\rm SY}(r)$ is more suitable for the present purpose. The cross section calculated by $R_{\rm SY}(r)$ is given by

$$\sigma_{\rm SY} = \frac{\exp(2\mu r_0)}{1+\mu r_0}\frac{16\pi}{3}\frac{\hbar c}{(Mc^2)^2}e^2\left(\frac{Z}{A}\right)^2\frac{\sqrt{ES_n}}{E+S_n}, \qquad (8)$$

where the factor $\exp(2\mu r_0)/(1+\mu r_0)$ comes from the scaling of the Yukawa function mentioned above, and the rest is nothing but σ_Y. The cross section $\sigma_{\rm SY}$ is included in Figs. 1(a) and 1(b). One finds a good agreement between σ_W and $\sigma_{\rm SY}$ at lower E. Equation (8) indicates a $\sqrt{E}$ dependence for $E \ll S_n$, and is indeed seen also in σ_W and in the experiment [7]. This $\sqrt{E}$ dependence is reported in Ref. [7] as a puzzling phenomenon, but is now understood naturally. In the present case, $\exp(2\mu r_0)/(1+\mu r_0) \sim 4$, resulting in $\sigma_{\rm SY} \sim 4\sigma_Y$. This scaling law holds as a good approximation to σ_W for low E, whereas Fig. 1(b) shows that the scaling law breaks down at higher E where the inner part of $R(r)$ becomes more important.

By inspecting Fig. 2, one sees that the major part of $E1$ transition takes place, for a lower value of k, outside the usual nuclear radius. In other words, the halo or tunneling part of the wave function carries a dominant fraction of such low-energy $E1$ transitions. This is the basic mechanism for the Yukawa scaling law mentioned above.

The present result is obtained with $\zeta_1 = 1$. Since the S factor of the $2s_{1/2}$ orbit is given by $S \equiv \zeta_1^2$, one can determine the S factor from a fit in Fig. 1, as $S \sim 1.0$ with an error ~ 0.1. Since $|S| \le 1$, the S factor is evaluated in this study as $S \approx$0.9–1.0. The data in Fig. 1 [7] involve two sources of uncertainties, vertical and horizontal. The vertical errors are shown in Fig. 1. The horizontal uncertainty means that, since the energy is actually an average over a few tens keV [7], the energy values may have uncertainties up to about ten keV. Although the S factor may be somewhat smaller than 0.9 due to this horizontal uncertainty, these uncertainties are minor, and one can still determine rather accurately the S factor from Fig. 1. The presently fitted range of the S factor includes the value estimated by Kurath [5], whereas this range excludes a value indicated by Ohnuma *et al.* based on (d,p) reaction data [6]. We would like to emphasize that the direct capture is a very useful tool for measuring the S factor of a halo orbit, because the interaction is electromagnetic and therefore has no particular sensitivity to a specific region in contrast to hadronic probes. We also mention that the effective charge is rather well established for $E1$ transitions. Note that anomalies found in other reactions may be due to halo [6,8].

Although $R_W(r)$ reproduces the experiment well, it is empirical to a large extent. We can use a wave function obtained by a microscopic approach called the variational shell model (VSM) [3]. Figure 2 shows that $Q(r)$ for this function is nearly identical to $Q_W(r)$ with $r_0 = 4$ fm. This is one of the reasons why $r_0 = 4$ fm is taken. The VSM wave function produces almost the same cross section as this $R_W(r)$.

The continuum plane-wave states have overlaps with bound states, in general. These overlaps have to be removed in the calculation of continuum-to-bound matrix elements so that bound-to-bound transitions are not included. As the lowest order approximation, we orthogonalize $e^{i\mathbf{k}\cdot\mathbf{r}}$ to bound wave functions: $e^{i\mathbf{k}\cdot\mathbf{r}} - \sum_i |i\rangle\langle i|e^{i\mathbf{k}\cdot\mathbf{r}}\rangle$ where $|i\rangle$ means the ith bound orbit. Resultant wave functions are not orthonormalized, but the double counting is removed and the $E1$ sum rule from a bound orbit becomes correct. Although the effect of orthogonalization is incorporated only approximately by this method, one sees later that this effect is rather negligible in the region of interest. In a more refined treatment, the bound and continuum wave functions should be solved within a single framework. Figure 1(b) includes the cross section obtained from $R_W(r)$ with this orthogonalization, showing no significant difference at lower E from the result without the orthogonalization.

It is of interest to use another wave function, $R_{\rm HO}(r)$, obtained from the harmonic oscillator potential. Figure 1(b) includes the cross section calculated from $R_{\rm HO}(r)$ with the above orthogonalization, showing much smaller values. Figure 2 suggests that $R_{\rm HO}(r)$ produces a peak at higher E.

The $M1$ transition matrix element is proportional to the overlap of radial wave functions of initial and final states. The $M1$ transition occurs between orbits of the same orbital angular momentum. Therefore, unless one of the spin-orbit partners is in continuum, the $M1$ transition does not contribute to the direct capture. Thus, one cannot expect sizable $M1$ contribution in the present case.

The reversed process of the direct neutron capture is the photodisintegration. One expects the same feature as above, enhancement of $E1$ excitation at low energy due to halo. We shall consider the $E1$ excitation to continuum from the anomalous ground state of ^{11}Be, restricting ourselves to relatively low-energy neutron emission. Note that this state has a neutron halo [9]. The excitation energy in the c.m. frame is denoted as E. Other notations are the same as above. The energy derivative of $B(E1)$ is given by

$$\frac{dB(E1)}{dE} = \frac{M}{2\pi\hbar^2}k\frac{3}{4\pi}(Q_{1,0})^2, \qquad (9)$$

where $Q_{1,0}$ is defined in Eq. (5). The results are presented in Fig. 3 for $R_Y(r)$, $R_{\rm SY}(r)$, and $R_W(r)$ obtained with the observed value $S_n = 0.505$ MeV. For simplicity, $r_0 = 4$ fm is taken as similar to ^{13}C. In all cases, only the transition from the $2s_{1/2}$ orbit on the top of the ^{10}Be (0^+) core is considered. The other contributions involve more deeply bound orbits and/or higher core states, and do not contribute for low E. The magnitude is to be scaled by the actual value of the S factor or ζ_1^2. For instance, it is 0.65 in Ref. [10] and 0.55 in Ref. [3].

Figure 3 indicates that all results show a sharp increase

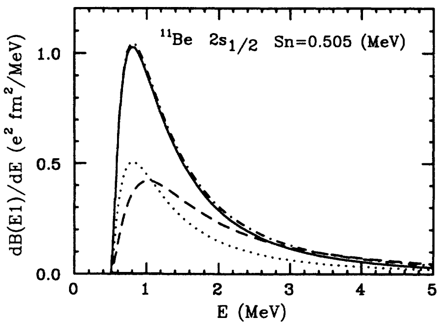

FIG. 3. $dB(E1)/dE$ for the photodisintegration of ^{11}Be as a function of the excitation energy E. The solid, dot-dashed, and dotted lines are obtained from R_W, R_{SY}, and R_Y, respectively. The dashed line is obtained from the VSM with the SIII interaction [3].

near the threshold. The $R_W(r)$ and $R_{SY}(r)$ wave functions produce almost identical peaks near the threshold, because only the tail part is relevant, which is practically common between $R_W(r)$ and $R_{SY}(r)$. In fact, one obtains the following analytic formula from $R_{SY}(r)$,

$$\frac{dB(E1)}{dE} = \frac{\exp(2\mu r_0)}{1+\mu r_0}\frac{3\hbar^2}{\pi^2 M} \times e^2\left(\frac{Z}{A}\right)^2 \frac{\sqrt{S_n}(E-S_n)^{3/2}}{E^4}. \qquad (10)$$

The peak is located at $E = \frac{8}{5}S_n$ with its height $\propto S_n^{-2}$ at $S_n \to 0$. The result obtained from $R_Y(r)$, where the scaling factor $\exp(2\mu r_0)/(1+\mu r_0)$ is missing, has been discussed in terms of the so-called cluster model for ^{11}Li [11]. This result has the same shape as the $R_{SY}(r)$ result but underestimates the whole magnitude by this factor, which is ~ 2 for ^{11}Be. Note that $R_Y(r)$ does not have sufficient amplitude outside the nuclear surface. Since the present quantity is sensitive almost entirely to the region outside the surface, the agreement between the result of $R_{SY}(r)$ and that of $R_W(r)$ persists up to higher E in comparison to the case of ^{13}C. More generally, for a halo state with a smaller S_n, the wave function of the last neutron becomes more strongly dominated by the portion outside the surface and hence the scaled Yukawa approximation becomes good in a wider region of E. The integrated $B(E1)$ for up to $E \sim 4$ MeV is about 1.2 e^2 fm^2 for $R_W(r)$. The $R_{SY}(r)$ is used for the analysis of the breakup of ^{11}Be by Anne *et al.* [12]. Figure 3 includes the result obtained from the VSM wave function, showing a broader peak. This is because the SIII interaction overestimates S_n of ^{11}Be by $\sim$ 0.4 MeV. This is not a significant energy deviation, but makes a crucial change in the tunneling effect as compared to the observed value $S_n = 0.505$ MeV. A refinement of the Skyrme force is needed for unstable nuclei.

As we have seen above, the $E1$ photodisintegration serves as a clear experimental device to identify the neutron halo structure in the ground state. We emphasize that the transitions around $r \sim 14$ fm mainly contribute to the peak in Fig. 3. Since the wave function of $r \sim 14$ fm is entirely due to tunneling, the restoring force is absent or very weak. Hence and also from the viewpoint of the shape, the peak is considered to be a nonresonant one, contrary to the expectation of soft $E1$ resonance [13]. As we mentioned at Eq. (10), the peak of $dB(E1)/dE$ near the threshold becomes gigantic as $S_n \to 0$. This is due to the increasing dipole transition moment as the halo extends with decreasing S_n. The peak energy is then lowered because the $E1$ transition occurs to p wave states with lower k values.

In summary, the halo formation (or tunneling) produces significant effects on the direct neutron capture and $E1$ photodisintegration as seen in ^{13}C and ^{11}Be, respectively, because the p-wave continuum states are strongly connected by $E1$ transition with the s orbit with halo.

We acknowledge Prof. Y. Nagai for his valuable discussions. We are grateful to Prof. A. Gelberg for a careful reading of the manuscript. This work was supported in part by Grant-in-Aid for General Scientific Research (No. 04804012) and by Grant-in-Aid for Scientific Research on Priority Areas (No. 05243102) from the Ministry of Education, Science and Culture. This work was supported partly by the Special Researchers' Basic Science Program at Riken. The VAX 6640 at the Meson Science Laboratory, the University of Tokyo, was used for computation.

[1] I. Tanihata *et al.*, Phys. Lett. **160B**, 380 (1985); I. Tanihata, Nucl. Phys. **A552**, 275c (1991).
[2] P. G. Hansen and B. Jonson, Europhys. Lett. **4**, 409 (1987).
[3] T. Otsuka, N. Fukunishi, and H. Sagawa, Phys. Rev. Lett. **70**, 1385 (1993).
[4] J. M. Blatt and V. F. Weisskopf, *Theoretical Nuclear Physics* (Wiley, New York, 1952).
[5] D. Kurath, Phys. Rev. Lett. **35**, 1546 (1975).
[6] H. Ohnuma *et al.*, Nucl. Phys. **A448**, 205 (1985).
[7] T. Ohsaki, Y. Nagai, M. Igashira, T. Shima, K. Takeda, S. Selno, and T. Irie, Astrophys. J. (to be published).
[8] K.-I. Kubo, K. G. Nair, and K. Nagatani, Phys. Rev. Lett. **37**, 222 (1976).
[9] M. Fukuda *et al.*, Phys. Lett. B **268**, 339 (1991).
[10] D. L. Auton, Nucl. Phys. **A157**, 305 (1970).
[11] C. A. Bertulani and A. Sustich, Phys. Rev. C **46**, 2340 (1992).
[12] R. Anne *et al.*, Phys. Lett. B **304**, 55 (1993).
[13] K. Ikeda, Nucl. Phys. **A538**, 355c (1992).